

Estimation of air velocity for a high velocity spinning projectile using transverse accelerometers

Aurélien Fiot* , Sébastien Changey† and Christophe Combettes‡

French-German Research Institute of Saint-Louis ISL, France

Nicolas Petit§

MINES ParisTech, PSL Research University, France

In this article, we propose a method to estimate the velocity of a projectile from strap-down transverse accelerometers. The ballistic projectile under consideration has a high velocity and a high spin rate. The transverse accelerometers measure the aerodynamics forces in a frame that is oscillating due to the pitching and yawing motion. We exploit the linearized pendulum-like equations of motion of the rotation dynamics to determine the frequencies contained in the spectrum of the measurements. Analytically, we show that three frequencies are present, the expressions of which explicitly contain the air velocity. Further, it is shown that, for the most part of the flight, only one frequency is truly visible. Extracting the value of this frequency from accelerometer signals can be performed over short time windows with a super resolution algorithm. Eventually the velocity can be estimated from an inversion of the analytic formula of the theoretical value of the frequency obtained from the aerodynamic model of the projectile. Realistic simulation results are presented, stressing the relevance of the approach, along with perspectives on the treatment of real in-flight data.

Nomenclature

M	Mass of the projectile ($M = 44.997$ kg)
D	Caliber of the projectile ($D = 0.155$ m)
I_l	Longitudinal moment of inertia of the projectile ($I_l = 0.1537$ kg.m ²)
I_t	Transverse moment of inertia of the projectile ($I_t = 1.812$ kg.m ²)
x	Coordinate along the horizontal axis of the shot
y	Altitude coordinate
z	Deviation coordinate
η	Horizontal angle from the shot main axis to the projection of the velocity of the projectile on the horizontal plane
θ	Vertical angle from the direction defined by η to the velocity of the projectile
β	Horizontal angle from the velocity of the projectile to the projection of its main direction on the plane defined by η and θ
α	Vertical angle from the direction defined by β to the projectile's main direction
φ	Angle describing the roll of the projectile around its main axis in the trajectory frame
v	Linear velocity of the projectile
Ω	Angular velocity $\Omega = (p, q, r)$ (for fast-spinning projectiles $ \Omega \simeq p \simeq \dot{\varphi} $)

*PhD candidate at MINES ParisTech, Guidance, Navigation and Control department at ISL

†Dr. Eng., Guidance, Navigation and Control department at ISL

‡Dr. Eng., Guidance, Navigation and Control department at ISL

§Professor, CAS - Centre automatique et systèmes, 60 bd St Michel 75006 Paris, AIAA Senior Member.

I. Introduction

This article exposes a method to estimate the linear velocity of a high velocity spinning ballistic projectile (shell). The problem under consideration deals with the general question of full state (6 DOF) estimation for the next generation of shells (so-called “smart shells”, a prime example being Raytheon’s Excalibur), that will contain various types of sensors. Commonly, such solid body can be equipped with low-cost inertial sensors, which as is well known,¹⁻⁷ can be used to reliably solve the navigation problem, at the expense of reasonably complex on-board calculations and off-line tasks such as calibration of the multi sensor system.⁸ Various experiments have been reported in the literature for UAVs,⁹⁻¹¹ UGVs,¹² micro-satellites,¹³⁻¹⁵ sounding rockets,¹⁶ spacecrafts¹⁷⁻¹⁹ among others. Similar ideas are being transposed to the case of shells. However, shells have some particular features that significantly impact the nature of the navigation problem.

The trajectory of a shell is short due to its high speed, and (almost always) subjected to a high spinning rate (in the roll direction).²⁰⁻²² The spin is voluntarily created to stabilize the trajectory of the shell and to reduce the impact of side wind. First, the short duration of the flight causes problem to GPS sensors, which usually work at low measurement rates. A typical flat shot lasting less than 2 sec on a proving ground, while a ballistic shot would last less than 45 sec, this leaves the 2-6 Hz GPS receiver little time to produce reliable information. Furthermore, the spin discards the low-cost gyrometers from being used. Typically, rotation rates of 300 Hz are considered, which is out of the scale of most low-cost gyrometers. Finally, gyrometers are prone to be damaged by the high impact the shell is subjected to right during the shot. Unfortunately, gyrometers are a key element in navigation algorithms.²³⁻²⁵ These facts make the navigation problem for shells a difficult one.

In this article we propose a method, that is unusual, to solve one central question in navigation of shells: the estimation of its linear velocity. The method takes advantage of the oscillations the shell is subjected to. It uses transverse accelerometers signals to generate a roll-free signal which measures the yaw and pitch coupled dynamics. This pendulum-like rotation dynamics is created by aerodynamics effects in a way that is well modeled. Rather than simply inverting aerodynamics lookup tables (e.g. inverting the measurement of the drag to estimate the velocity through an estimate of the dynamic pressure), we estimate frequencies and deduce the value of the linear velocity from this estimate. The technique employs frequency detection algorithms (*super-resolution*²⁶) that are well suited for the signal generated during the ballistic flight. The results presented in this article show the potential of the method which is tested on simulation data. It is shown that during most of the ballistic flight, the linear velocity can be recovered with a good level of accuracy. At the end of the paper, some perspectives are given for further studies in view of application to real flight data.

II. Model

II.A. The shell

The projectile under consideration is a 155 mm caliber shell equipped with several sensors (three-axis magnetometers, 3-axis accelerometer), a data transmitter with its antenna, and batteries. No gyrometers are embedded due to the harshness of the environment (the shot generates a 15.000 g acceleration which would cause serious damages to the gyrometers, not to mention the spin rate of 300 rotation per second the gyrometers would need to endure). A schematic view of such a “smart-shell” (with smaller size) is reported in Figure 1, more details are given in²⁷.

II.B. Model

Classically, several frames of reference are used. The notations are given in the Nomenclature section. The two important reference frames in the model of the equations of motion we consider are the inertial (ground) frame and the trajectory frame $(\vec{t}, \vec{s}, \vec{h})$. The trajectory frame is defined with one axis co-linear to the velocity vector of the shell, and the two other axis being defined with the rotations described in Figures 2,3.

Usually, the body frame is defined from the inertial frame with the 3 Euler angles of aeronautics (the yaw, pitch and roll angles), and thus 2 angles are needed to relate the body frame to the trajectory (the angle of attack α_{aero} and the sideslip angle β_{aero}). Here, we consider 2 angles to define the trajectory frame within the inertial frame (η and θ), and thus 3 angles are needed to represent the body frame in the trajectory

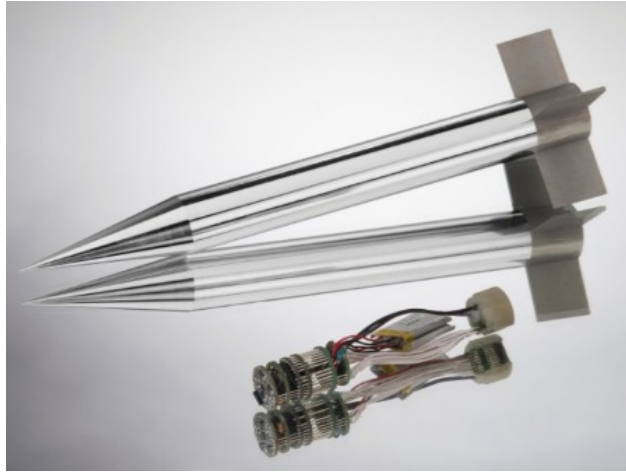


Figure 1. An Institut Saint-Louis smart-shell with its sensors and data transmitter.

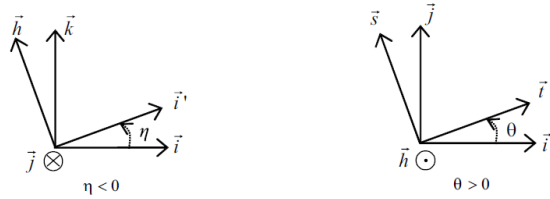


Figure 2. Trajectory frame definition

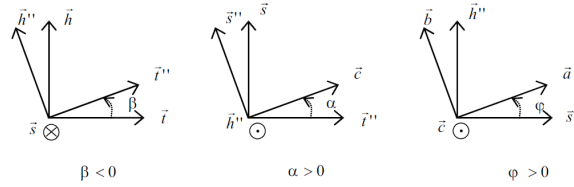


Figure 3. Body frame definition

frame : α and β , representing the pitching and yawing motion in the trajectory frame, and φ , representing the rolling motion in the trajectory frame.^a

The 3-axis accelerometer, when precisely located at the center of mass of the shell, produces the following three signals

$$\begin{aligned}
 A_c &\simeq A_{acc} \\
 A_a &\simeq -\frac{D+L}{M}\beta_{aero} + \frac{K}{M}\alpha_{aero} \\
 A_b &\simeq -\frac{D+L}{M}\alpha_{aero} + \frac{K}{M}\beta_{aero}
 \end{aligned} \tag{1}$$

where A_{acc} is the ratio of the norm of the vector of aerodynamic forces and the mass, and D, L, K the norms of the Drag, Lift and Magnus forces.

The high spin rate has a major effect on the two signals A_a and A_b from the transverse accelerometers. However, a simple sum of squares of these two signals in quadrature provides a signal of interest

$$f(t) = A_a^2(t) + A_b^2(t) = A_{acc}^2(t)(\alpha^2(t) + \beta^2(t)) \tag{2}$$

^aNote that α_{aero} and β_{aero} are related to α and β , through a rotation matrix of angle φ .

Interestingly, the two angles α and β satisfy coupled dynamics that are detailed below.

Under the assumptions that the linear velocity, and the trajectory angles η and θ are slowly varying, and if the angles α and β are small, then the complex valued variable

$$\xi(t) = \alpha(t) + i\beta(t)$$

satisfies the so-called equation of ballistics (see²⁸ and references therein) (3).

$$\ddot{\xi} + \frac{v}{D} (a_1 - ib_1)\dot{\xi} + \frac{v^2}{D^2}(a_2 - ib_2)\xi = \frac{v^2}{D^2}(a_3 - ib_3) \quad (3)$$

where the a_i and b_i are depending on the linear velocity, the angular velocity, the aerodynamics coefficients at zero angles of attack and the altitude (through the dependance of the air density). Detailed expressions can be found in Appendix. Equation (3) defines a complex-valued damped oscillator.

III. Frequency content of the transverse accelerometers signals

The signals from the two transverse accelerometers have been lumped into $f(t)$ through (2). A careful resolution of the ballistic equation (3) allows one to decompose its solution as the sum of three terms, among which two are damped oscillating terms. In details, using two constant complex coefficients $\underline{\lambda}_1$ and $\underline{\lambda}_2$ depending on the initial conditions, one has, on a window small enough for the coefficients of (3) to be regarded as constant,

$$\xi(t + \delta t) = \frac{a_3 - ib_3}{a_2 - ib_2} + \underline{\lambda}_1 f_1(\delta t) e^{i\omega_1 \delta t} + \underline{\lambda}_2 f_2(\delta t) e^{i\omega_2 \delta t} \quad (4)$$

with

$$f_1(\delta t) = e^{\frac{v}{2D}(a_1 - M_1)\delta t}, \quad f_2(\delta t) = e^{\frac{v}{2D}(a_1 + M_1)\delta t}, \quad \omega_1 = \frac{v}{2D}(b_1 + M_2), \quad \omega_2 = \frac{v}{2D}(b_1 - M_2)$$

where M_1 and M_2 are the uniquely defined strictly positive reals such that

$$(M_1 + iM_2)^2 = (a_1^2 - b_1^2 - 4a_2) + i(4b_2 - 2a_1b_1)$$

namely

$$M_1 = - \left[(a_1^2 - b_1^2 - 4a_2)^2 + (4b_2 - 2a_1b_1)^2 \right]^{\frac{1}{4}} \sin \left[\frac{1}{2} \arctan \left(\frac{4b_2 - 2a_1b_1}{a_1^2 - b_1^2 - 4a_2} \right) \right]$$

$$M_2 = \left[(a_1^2 - b_1^2 - 4a_2)^2 + (4b_2 - 2a_1b_1)^2 \right]^{\frac{1}{4}} \cos \left[\frac{1}{2} \arctan \left(\frac{4b_2 - 2a_1b_1}{a_1^2 - b_1^2 - 4a_2} \right) \right]$$

It appears that, once squared to compute the norm of $\xi(t)$ appearing in (2), the two frequencies appearing in (4) give rise to three damped oscillating terms. In details, one has

$$f(t) = A_{acc}^2 \left[\left| \frac{a_3 - ib_3}{a_2 - ib_2} \right|^2 + 2|\underline{\lambda}_1|^2 f_1(t)^2 + |\underline{\lambda}_2|^2 f_2(t)^2 + \sum_{i=1}^3 C_i f_i(t) \cos(\omega_i t + \phi_i) \right] \quad (5)$$

The three frequencies $\omega_1 > \omega_3 > \omega_2$ contained in this signal are

$$\omega_1 = \frac{v}{2D}(b_1 + M_2), \quad \omega_3 = \frac{v}{D}M_2, \quad \omega_2 = \frac{v}{2D}(b_1 - M_2) \quad (6)$$

In this expression, ω_1 and ω_2 are functions of the linear velocity, the roll velocity (and the altitude). We now assume that the dependency on the altitude can be neglected (this is particularly true for flat fires) or compensated for (using an estimate of the altitude, which, in turn, could be obtained by integrating the linear velocity without too much uncertainty as the initial conditions are certain). We also consider that the roll velocity is known. As already mentioned in the introduction of the article, no gyrometers are embedded in our shell, therefore an alternative solution is required. For this, the task of estimating the angular velocity of the rigid body can be solved using the embedded magnetometers which serve here as direction sensors, through a state observer.^{29,30} Alternatively, a frequency analysis of the magnetometers signal can also be used.

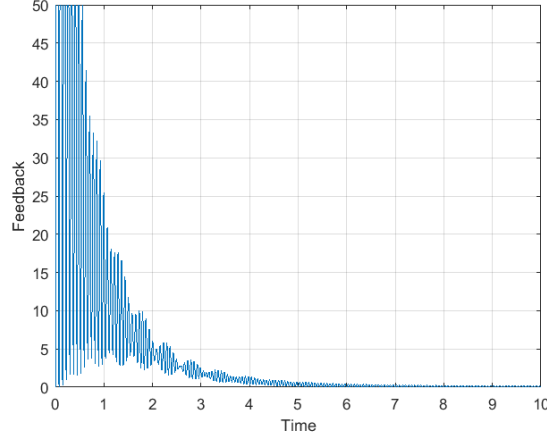


Figure 4. Accelerometric signal $f(t)$ from simulation data

IV. Spectrum analysis: frequency detection

A common practice to estimate the frequency of a monochromatic signal (or a multisinusoidal signal) is Fast Fourier Transform (FFT). This technique, at the heart of the *periodogram* technique, is often employed in various applicative situations such as target identification from radar measurements, acoustics, among others. The FFT is well suited for cases where a relatively large window can be used to estimate the frequency.³¹ This is necessary to avoid boundary effects, spectral aliasing, and frequency leak^{31b}. This is not the case in the application considered here, because the signal is decaying over time. Employing a large window violates the assumption that the signal has constant magnitude, which is implicitly required for the FFT technique to produce quality results.

Fortunately, alternative solutions exist. We use the *super-resolution* technique recently developed.³² In a nutshell, this technique is optimization-based (in the time domain), as it seeks the frequencies of a multisinusoidal signal as the solution of a best-fit problem. Various implementations exist, e.g. Prony based methods (MUSIC³³) and total-variation norm minimization methods.²⁶ On top of improving resolution (as the name of *super-resolution* suggests it), the methods have proven capabilities of outlier rejection even with high noise/signal ratios. To work effectively, *super-resolution* methods require that the numbers of frequencies to be located in the signal be known in advance. This is precisely the case in our application. Based on the previous modeling and calculus, we know that the signal derived from the transverse accelerometers contains 1 or 3 frequencies to be detected. *Super-resolution* methods can deal with short time windows, typically half a period of the lowest frequency to be detected is enough. This is a very helpful feature in our case.

V. Filtering the velocity from spectrum measurements

As we showed, precession frequencies dependencies on the velocity are well known ;

$$\begin{aligned} \omega_1(v, p, y) &= \frac{p}{2} \frac{I_l}{I_t} + \frac{v}{2D} [(a_1^2 - b_1^2 - 4a_2)^2 + (4b_2 - 2a_1b_1)^2]^{\frac{1}{4}} \cos \left[\left(\frac{1}{2} \arctan \left(\frac{4b_2 - 2a_1b_1}{a_1^2 - b_1^2 - 4a_2} \right) \right) \right] \\ \omega_2(v, p, y) &= \frac{p}{2} \frac{I_l}{I_t} - \frac{v}{2D} [(a_1^2 - b_1^2 - 4a_2)^2 + (4b_2 - 2a_1b_1)^2]^{\frac{1}{4}} \cos \left[\left(\frac{1}{2} \arctan \left(\frac{4b_2 - 2a_1b_1}{a_1^2 - b_1^2 - 4a_2} \right) \right) \right] \\ \omega_3(v, p, y) &= \frac{v}{D} [(a_1^2 - b_1^2 - 4a_2)^2 + (4b_2 - 2a_1b_1)^2]^{\frac{1}{4}} \cos \left[\left(\frac{1}{2} \arctan \left(\frac{4b_2 - 2a_1b_1}{a_1^2 - b_1^2 - 4a_2} \right) \right) \right] \end{aligned}$$

One can thus easily design an estimator of the velocity from measurements of those frequencies, using the roll rate p and the altitude y as external outputs.

^bAn intrinsic weakness of the FFT-based technique is its coarse resolution, i.e. the relevant frequencies are located with a poor resolution. This is a problem in our case.

VI. Results

The signal stemming from the transverse accelerometers is treated using the MUSIC algorithm. The signal is obtained from a reference simulation model. It consists of regularly spaced samples obtained at 10^4 Hz. The MUSIC algorithm is run on moving windows of 0.2 s and 2 s (to adapt respectively to ω_1 and ω_2). By contrast with FFT-based techniques, no smoothing nor filtering of the data is performed. MUSIC is set-up to search for a single frequency. The results of the frequency detection are reported in Figure 5 and Figure 6. In this figure, the true value of the frequencies ω_1 and ω_2 are given for comparisons with the estimation obtained from MUSIC. As one can see, whereas ω_1 is detected with great accuracy due to being visible in small windows on which its value does not vary much (although it vanishes after the peak altitude of the trajectory), ω_2 is on the other hand being detected during the whole flight, but with poor accuracy due to the large windows needed for its detection.

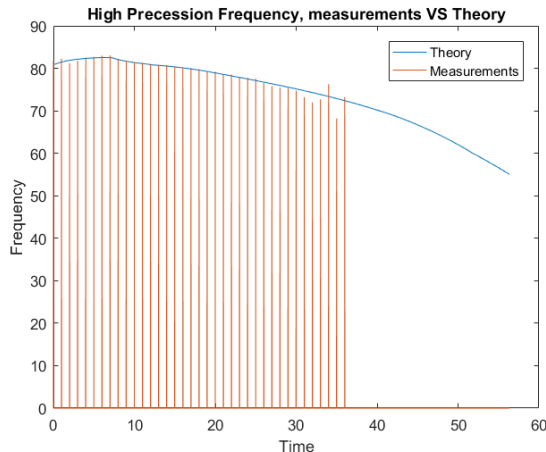


Figure 5. Estimate of the highest frequency ω_1 in the signals obtained from the transverse accelerometers measurements

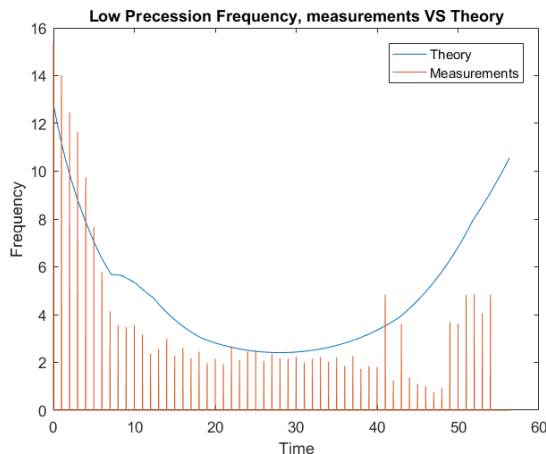


Figure 6. Estimate of the lowest frequency ω_2 in the signals obtained from the transverse accelerometers measurements

Based on the previous frequency detection, the linear velocity can be estimated with a filter based on from the closed-form expression (7). We chose to use only ω_1 , as its detection is the most accurate, and given that the filter can be made convergent before ω_1 vanishes.

$$\omega_1(v, p, y) = \frac{p}{2} \frac{I_l}{I_t} + \frac{v}{2D} [(a_1^2 - b_1^2 - 4a_2)^2 + (4b_2 - 2a_1b_1)^2]^{\frac{1}{4}} \cos \left[\left(\frac{1}{2} \arctan \left(\frac{4b_2 - 2a_1b_1}{a_1^2 - b_1^2 - 4a_2} \right) \right) \right] \quad (7)$$

The filter yields the velocity estimation reported in Figure 7, and produces quite satisfying result given a 20% initial error. We chose not to display the result of the filter using both ω_1 and ω_2 measurements ; its

result are quite bad, which is not surprising when one look at the poor detection of ω_2 used.

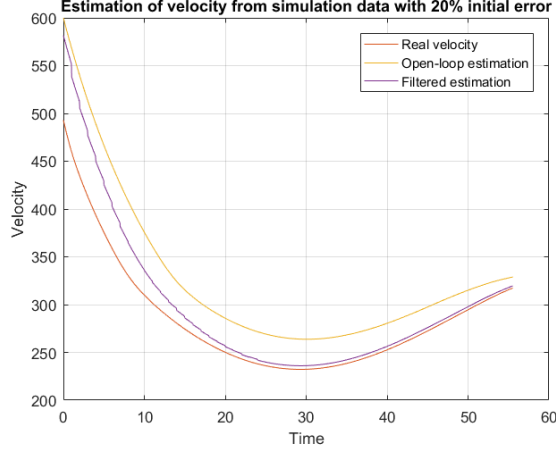


Figure 7. Estimates of the shell linear velocity from shot to target reaching.

VII. Conclusion and perspectives

In this paper we have exposed the principles of a novel technique which uses the signal from transverse accelerometers to estimate the linear velocity of a high velocity spin projectile (shell). This technique is very different from existing ones, e.g. the use of axial accelerometer to estimate the linear velocity from inversion of the drag model (similarly to Pitot sensors). Here, we exploit the coupled pitching and yawing dynamics and estimate the linear velocity through the dependency of the natural frequency of these coupled pendulum-like dynamics. Interestingly, the numerical treatment that are employed are, by nature, robust to faulty data. However, several difficult points can be anticipated in view of practical applications. Preliminary investigations of actual data recorded during test shots reveal that the signals from the transverse accelerometers is corrupted not only by noises, which to some extent are not troubling our method, but by parasitic sensed motions caused by their locations inside the shell. By contrast with the assumption formulated in this article, the transverse accelerometers are not located at the center of mass, but slightly away from it (at a distance of 0.1 mm). This distance can be quite accurately measured, but because the rotation rate of the shell is very high (typically 300 Hz), the error in the transverse accelerometers measurement is still not negligible and difficult to reduce in the presence of sensors misalignment and scale factors. The method described in this paper can actually be extended easily by using the feedback from only one transverse accelerometer, as it is shown that the significant (regarding amplitude) inertia terms yields the same frequencies ($p - \omega_1$ and $p - \omega_2$) as an ideal transverse accelerometer.

Appendix

Below the expressions of coefficients appearing in the ballistic equation (3) are given.

$$\begin{aligned}
 a_1 &= -B_M C_{mq} + B_F (\hat{C}_{L\alpha} - \hat{C}_D), & a_2 &= -B_M \hat{C}_{M\alpha}, & a_3 &= \frac{gD \cos \theta}{v^2} (-B_M C_{mq} + B_F \hat{C}_D), \\
 b_1 &= \frac{p}{v} D \frac{I_l}{I_t}, & b_2 &= b_1 (B_F \hat{C}_{L\alpha} - B_M \hat{C}_{mag-m} \frac{I_t}{I_l}), & b_3 &= \frac{gD^2 \cos \theta}{v^3} p \frac{I_l}{I_t}, \\
 B_F &= \frac{\rho_a S D}{2m}, & B_M &= \frac{\rho_a S D^3}{2I_t}.
 \end{aligned}$$

The aerodynamic coefficients are functions of the Mach number and specific to the projectile considered. \hat{C}_D describes the drag force, $\hat{C}_{L\alpha}$ the lift force, \hat{C}_{mag-m} the Magnus moment, $\hat{C}_{M\alpha}$ the overturning moment, and C_{mq} the pitch-damping moment.

References

- ¹Shuster, M. D., "Approximate algorithms for fast optimal attitude computation," *Proceedings of the AIAA Guidance and Control Conference*, 1978, pp. 88–95.
- ²Bar-Itzhack, I. Y., "REQUEST - A New Recursive Algorithm for Attitude Determination," *Proceedings of the National Technical Meeting of The Institute of Navigation*, 1996, pp. 699–706.
- ³Choukroun, D., *Novel methods for attitude determination using vector observations*, Ph.D. thesis, Technion, 2003.
- ⁴Hamel, T. and Mahony, R., "Attitude estimation on SO[3] based on direct inertial measurements," *Proceedings 2006 IEEE International Conference on Robotics and Automation, 2006. ICRA 2006.*, May 2006, pp. 2170–2175.
- ⁵Crassidis, J. L., Markley, F. L., and Cheng, Y., "Survey of nonlinear attitude estimation methods," *Journal of Guidance, Control, and Dynamics*, Vol. 30, No. 1, 2007, pp. 12–28.
- ⁶Tayebi, A., McGilvray, S., Roberts, A., and Moallem, M., "Attitude estimation and stabilization of a rigid body using low-cost sensors," *Decision and Control, 2007 46th IEEE Conference on*, IEEE, 2007, pp. 6424–6429.
- ⁷Berkane, S., Abdessameud, A., and Tayebi, A., "A globally exponentially stable hybrid attitude and gyro-bias observer," *Decision and Control (CDC), 2016 IEEE 55th Conference on*, IEEE, 2016, pp. 308–313.
- ⁸Fourati, H. and Belkhiat, D. E. C., *Multisensor Attitude Estimation: Fundamental Concepts and Applications*, CRC Press, 2016.
- ⁹Metni, N., Pflimlin, J.-M., Hamel, T., and Souères, P., "Attitude and gyro bias estimation for a VTOL UAV," *Control Engineering Practice*, Vol. 14, No. 12, 2006, pp. 1511 – 1520.
- ¹⁰Jung, D. and Tsiotras, P., "Inertial Attitude and Position Reference System Development for a Small UAV," *AIAA Infotech at Aerospace*, 2007.
- ¹¹Hua, M. D., Ducard, G., Hamel, T., Mahony, R., and Rudin, K., "Implementation of a Nonlinear Attitude Estimator for Aerial Robotic Vehicles," *IEEE Transactions on Control Systems Technology*, Vol. 22, No. 1, 2014, pp. 201–213.
- ¹²Skog, I. and Handel, P., "In-car positioning and navigation technologies – A survey," *IEEE Transactions on Intelligent Transportation Systems*, Vol. 10, No. 1, 2009, pp. 4–21.
- ¹³Sunde, B. O., *Sensor Modelling and attitude determination for micro-satellites*, Master's thesis, NTNU, 2005.
- ¹⁴Magnis, L. and Petit, N., "Rotation estimation for a satellite from Sun sensors," *Control Conference (ECC), 2013 European*, IEEE, 2013, pp. 852–859.
- ¹⁵Springmann, J. C., Sloboda, A. J., Klesh, A. T., Bennett, M. W., and Cutler, J. W., "The attitude determination system of the RAX satellite," *Acta Astronautica*, Vol. 75, 2012, pp. 120–135.
- ¹⁶Bekkeng, J. K. and Psiaki, M., "Attitude Estimation for Sounding Rockets Using Microelectromechanical System Gyros," *Journal of Guidance, Control, and Dynamics*, Vol. 31, No. 3, 2008, pp. 533–542.
- ¹⁷Lee, H., Choi, Y.-H., Bang, H.-C., and Park, J.-O., "Kalman Filtering for Spacecraft Attitude Estimation by Low-Cost Sensors," *KSAS International Journal*, Vol. 9, No. 1, 2008, pp. 147–161.
- ¹⁸Springmann, J. C. and Cutler, J. W., "Optimization of directional sensor orientation with application to photodiodes for spacecraft attitude determination," *Journal of Guidance, Control, and Dynamics*, Vol. 37, 2014, pp. 828–837.
- ¹⁹Springmann, J. C. and Cutler, J. W., "Flight results of a low-cost attitude determination system," *Acta Astronautica*, Vol. 99, 2014, pp. 201–214.
- ²⁰McCoy, R. L., *Modern exterior ballistics*, Schiffer, 2nd ed., 1998.
- ²¹Yu, J., Bu, X., Xiang, C., and Yang, B., "Spinning projectile's attitude measurement using intersection ratio of magnetic sensors," *Proceedings of the Institution of Mechanical Engineers, Part G: Journal of Aerospace Engineering*, 2016.
- ²²Changey, S., Pecheur, E., and Brunner, T., "Attitude estimation of a projectile using magnetometers and accelerometers, experimental validation," *Position, Location and Navigation Symposium - PLANS 2014, 2014 IEEE/ION*, 2014, pp. 1168–1173.
- ²³Titterton, D. and Weston, J., *Strapdown Inertial Navigation Technology*, The American Institute of Aeronautics and Astronautics, Reston, USA, 2nd ed., 2004.
- ²⁴Crassidis, J. L., Markley, F. L., and Cheng, Y., "Survey of nonlinear attitude estimation methods," *Journal of Guidance, Control and Dynamics*, 2007.
- ²⁵Zarchan, P., *Tactical and Strategic Missile Guidance*, The American Institute of Aeronautics and Astronautics, 2007.
- ²⁶Fernandez-Granda, C., Tang, G., Wang, X., and Zheng, L., "Demixing Sines and Spikes : Robust Spectral Super-resolution in the Presence of Outliers," *Information and Inference*, sep 2017.
- ²⁷Changey, S., Pecheur, E., Bernard, L., Sommer, E., Wey, P., and Berner, C., "Real time estimation of projectile roll angle using magnetometers: In-flight experimental validation," *Position Location and Navigation Symposium (PLANS), 2012 IEEE/ION*, 2012, pp. 371–376.
- ²⁸Changey, S., *Modélisation et estimation par filtrage non linéaire, de l'attitude d'un projectile à partir de magnétomètres*, Ph.D. thesis, Supelec, 2005.
- ²⁹Magnis, L. and Petit, N., "Angular Velocity Nonlinear Observer from Single Vector Measurements," *Automatic Control, IEEE Transactions on*, Vol. 61, No. 9, 2016, pp. 2473–2483.
- ³⁰Magnis, L. and Petit, N., "Angular velocity nonlinear observer from vector measurements," *Automatica*, Vol. 75, 2017, pp. 46–53.
- ³¹Mallat, S., *A wavelet tour of signal processing: the sparse way*, Academic Press, 2008.
- ³²Fernandez-Granda, C. and Candès, E. J., "Towards a mathematical theory of super-resolution," *Communications on Pure and Applied Mathematics*, Vol. 67, No. 6, 2014, pp. 906–956.